Current Biology 21, 1480–1487, September 13, 2011 ©2011 Elsevier Ltd All rights reserved DOI 10.1016/j.cub.2011.07.040

Report

# Dscam1-Mediated Self-Avoidance Counters Netrin-Dependent Targeting of Dendrites in *Drosophila*

**Benjamin J. Matthews[1] and Wesley B. Grueber[1,2,*]**
[1]Department of Neuroscience
[2]Department of Physiology and Cellular Biophysics
College of Physicians and Surgeons, Columbia University,
630 West 168th Street, P&S 11-511, New York, NY 10032, USA

## Summary

**Dendrites and axons show precise targeting and spacing patterns for proper reception and transmission of information in the nervous system. Self-avoidance promotes complete territory coverage and nonoverlapping spacing between processes from the same cell [1, 2]. Neurons that lack *Drosophila* Down syndrome cell adhesion molecule 1 (Dscam1) show aberrant overlap, fasciculation, and accumulation of dendrites and axons, demonstrating a role in self-recognition and repulsion leading to self-avoidance [3–11]. Fasciculation and accumulation of processes suggested that Dscam1 might promote process spacing by counterbalancing developmental signals that otherwise promote self-association [9, 12]. Here we show that Dscam1 functions to counter *Drosophila* sensory neuron dendritic targeting signals provided by secreted Netrin-B and Frazzled, a netrin receptor. Loss of Dscam1 function resulted in aberrant dendrite accumulation at a Netrin-B-expressing target, whereas concomitant loss of Frazzled prevented accumulation and caused severe deficits in dendritic territory coverage. Netrin misexpression was sufficient to induce ectopic dendritic targeting in a Frazzled-dependent manner, whereas Dscam1 was required to prevent ectopic accumulation, consistent with separable roles for these receptors. Our results suggest that Dscam1-mediated self-avoidance counters extrinsic signals that are required for normal dendritic patterning, but whose action would otherwise favor neurite accumulation. Counterbalancing roles for Dscam1 may be deployed in diverse contexts during neural circuit formation.**

## Results and Discussion

### Elimination of Dendritic Self-Avoidance Reveals Focal Dendrite Targets for Dendritic Arborization Sensory Neurons

Dendritic territory formation involves both specific dendritic targeting and the spreading of branches across their target region. These processes are likely to be closely coordinated in time but under at least partially distinct molecular control by attractive and repulsive cues. To examine how these steps in territory formation are coordinated in individual arbors, we assessed the consequences of loss of Dscam1 on dendritic targeting of dendritic arborization (da) neurons. Sister dendrites of wild-type neurons rarely cross each other and thus spread evenly over their field (Figure 1A) [13], whereas dendrites of *Dscam1* mutant sensory neurons aberrantly cross, fasciculate, and accumulate (Figures 1B and 1C) [9–11]. Sites of accumulation could correspond to preferred targets of sister dendrites that are revealed absent the spacing constraints of self-avoidance [9]. To characterize the targets that may be responsible for dendrite accumulation, we focused on class III da neurons (ddaA and ldaB) that project dendrites near a peripheral sensory organ, the lateral chordotonal organ (LCHO) (Figure 1D) [9, 13]. Labeling of *Dscam1* clones, together with anti-HRP (horseradish peroxidase), anti-βPS-integrin, or anti-α-tubulin to label surrounding cells, revealed accumulations of dendrites at a distal region of CHO cap cells, a type of support cell that links CHO sensory neurons to the body wall (Figures 1E and 1F; see also Figure S1A available online) [14]. For simplicity, we refer to this targeted zone of cap cells as the lateral focus (LF). Branch density was higher at LF than the rest of the field in *Dscam1* clones (Figures 1G and 1H). Importantly, CHOs are positioned differently in thoracic and abdominal body segments; nevertheless, dendrites of *Dscam1* mutant sensory neurons accumulated at CHO cap cells regardless of their precise position (Figure S1B), strongly suggesting that it is this specific cell type, rather than other nearby cells, that directs targeting. Accumulations of dendrites in *Dscam1* mutant clones represented excessive targeting rather than an abnormal ectopic targeting event, because single dendrites of wild-type ddaA neurons also targeted precisely to LF at each larval instar (Figures 1I–1K; Figures S1C–S1F). These data together suggest that Dscam1 prevents excessive targeting of dendritic branches at peripheral cells that normally provide targeting instructions to sensory dendrites.

### Targeting of Sensory Dendrites Requires Frazzled

Dscam1 shows homophilic binding activity [15, 16] and in addition can serve as a receptor for the secreted netrins [17–19]. However, because dendrites showed robust targeting both in the presence and absence of Dscam1, we inferred that a signal for an alternate receptor is presented at LF. In a candidate screen of possible attractive receptors for LF targeting, we identified another netrin receptor, Frazzled/Deleted in Colorectal Cancer (Fra/DCC) [20–25]. Whereas wild-type ddaA clones showed robust targeting of a single branch to LF (Figures 2A and 2C), *frazzled*$^{3}$ (*fra*$^{3}$) mosaic analysis with a repressible cell marker (MARCM) clones showed significant disruptions in targeting (Figures 2B and 2C). Importantly, coincident loss of Frazzled suppressed the accumulation phenotypes seen in *Dscam1*$^{-/-}$ neurons (*Dscam1*$^{-/-}$ = 100% accumulated, n = 8; *Dscam1*$^{-/-}$, *fra*$^{-/-}$ = 0% accumulated, n = 13; Figure 2D). These data are consistent with a cell-autonomous role for Frazzled in sensory dendrite targeting and suggest that Dscam1 prevents excessive Frazzled-dependent targeting by sister dendrites.

We asked whether Dscam1 and Frazzled control larger-scale patterning of sensory neuron territories in addition to precise targeting. Modified Sholl analysis of the anterior-posterior arborization of ddaA indicated that wild-type arbors are polarized toward LF and have a relatively sparse anterior arborization (Figure 2E). We observed an anterior shift of ddaA territories (increased anterior and decreased posterior

*Correspondence: wg2135@columbia.edu

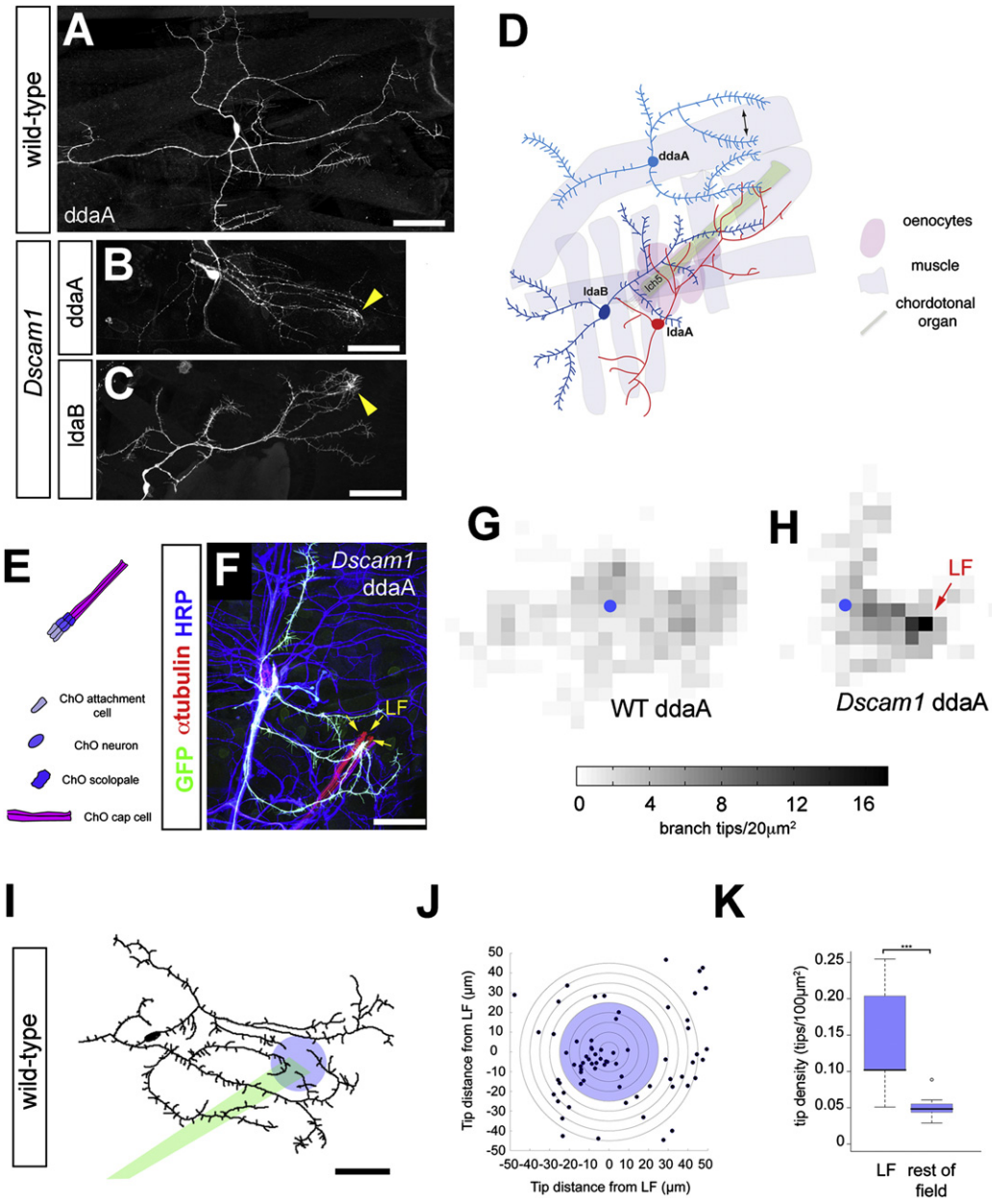


Figure 1. Targeting of *Dscam1* Mutant and Wild-Type Neurons to Chordotonal Organs

(A) Wild-type (WT) mosaic analysis with a repressible cell marker (MARCM) clone of the class III neuron ddaA. Sister dendrites show robust self-avoidance.

(B) *Dscam1*$^{21}$ mutant MARCM clone of class III neuron ddaA shows branch overlap and dendrite accumulation (yellow arrowhead).

(C) *Dscam1*$^{23}$ mutant MARCM clone of class III neuron ldaB shows branch overlap and dendrite accumulation (yellow arrowhead).

(D) Schematic of dendritic arborization (da) neurons and nearby nonneuronal cells, including muscle, oenocytes, and chordotonal organs. Epidermal cells upon which dendrites grow are not included in the schematic.

(E) The lateral chordotonal organ (LCHO) consists of a distal cap cell, scolopale cell, neuron, and proximal attachment cell.

(F) Labeling of a *Dscam1*$^{21}$ mutant ddaA MARCM clone with anti-GFP, anti-α-tubulin, and anti-HRP (horseradish peroxidase) reveals accumulation at the distal margin of LCHO in abdominal segments, termed the lateral focus (LF; yellow arrows).

(G) Density plot of all ddaA dendritic termini for wild-type (n = 8) MARCM clones. The average numbers of branch endings per cell that terminate within each 20 μm$^2$ square are plotted, with higher terminal density indicated by increasing grayscale. Blue circle indicates the position of the cell body.

(H) Density plot of ddaA dendritic termini for *Dscam1* MARCM clones (n = 4). The average numbers of branch endings per cell that terminate within each 20 μm$^2$ square are plotted as in (G). Blue circle indicates the position of the cell body. The accumulation of dendrite tips at LF in *Dscam1* mutant clones is indicated by a red arrow.

(I) Tracing of a wild-type ddaA neuron labeled with *189Y-Gal4, UAS-mCD8::GFP*. A green bar indicates the trajectory of the lateral chordotonal organ (LCHO). A blue circle with a 25 μm radius is centered at LF.

(J) Dendritic tips of ddaA in wild-type larvae are enriched within a 25 μm radius of LF when branch tips of multiple cells (n = 11) are plotted with respect to LF.

(K) The density of branch tips in a circle of radius 25 μm is significantly greater than the rest of the dendritic field.

All scale bars represent 50 μm. Data sets are presented in box plots as median (thick line), quartiles Q1–Q3 (25%–75% quantiles; shaded box), and data in 1.5× quartile range (dashed bars). Data points outside these ranges are indicated as open circles. *p < 0.05; **p < 0.01; ***p < 0.001 by Wilcoxon rank-sum test. See also Figure S1.

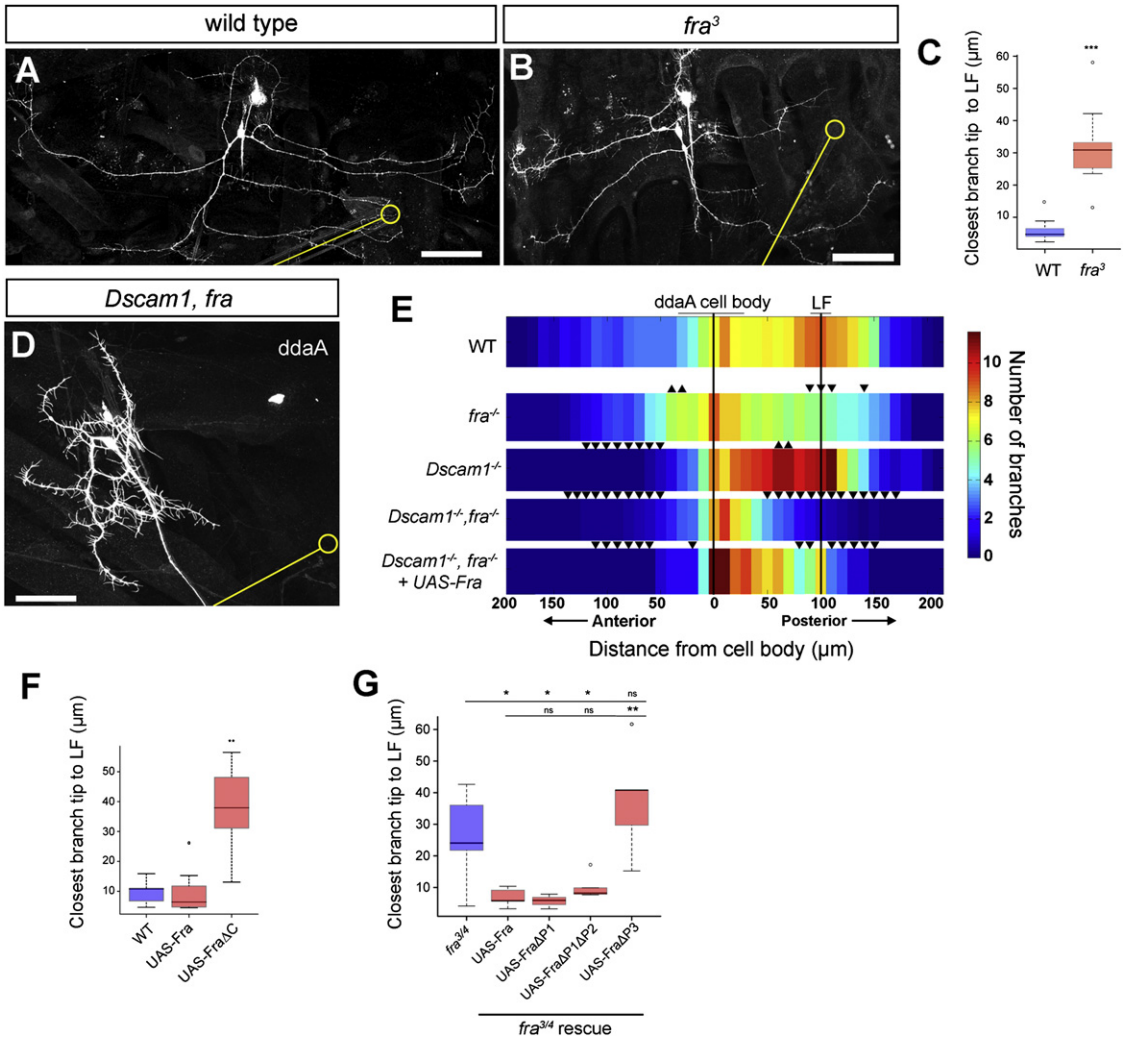


Figure 2. Frazzled Is Required for Sensory Neuron Dendrite Targeting

(A) A wild-type ddaA MARCM clone showing targeting of branches to the chordotonal organ. The chordotonal organ and LF are indicated by a yellow line and yellow circle, respectively, in this and subsequent panels.

(B) A *fra*$^{3}$ MARCM clone of ddaA showing disrupted targeting to LF.

(C) Plot of the distance of the closest branch tip to LF in wild-type (n = 8) and *fra*$^{3}$ (n = 9) mutant clones.

(D) Dendrites of *Dscam1*$^{21}$, *fra*$^{4}$ double mutant MARCM clone lack enrichment of dendritic termini at LF and show extensive dendritic clumping near the cell body.

(E) Horizontal Sholl analysis showing mean branch density values at 10 μm intervals for wild-type (n = 8), *fra* (n = 8), *Dscam1* (n = 5), *Dscam1*$^{21}$, *fra*$^{4}$ (n = 14), and *Dscam1*$^{21}$, *fra*$^{4}$ + *UAS-Fra* (n = 6) MARCM clones of ddaA. Upwards-pointing arrowheads denote significant increase in branch density relative to control ($p < 0.05$), whereas downwards-pointing arrowheads denote significant decrease in branch density ($p < 0.05$) as compared to topmost control strip.

(F) Quantification of the single closest branch tip to LF in control (n = 8), *UAS-Fra* (n = 7), and *UAS-Fra⊿C* (n = 6) FLP-out clones reveals no effect of *UAS-Fra* on targeting but a disruption of targeting caused by *UAS-Fra⊿C*. The pan-da neuron driver *109(2)80-Gal4* was used in these experiments.

(G) Quantification of closest branch tip to LF in FLP-out rescue experiments in *fra*$^{3}$/*fra*$^{4}$ mutant (n = 9) background. Introduction of *UAS-Fra* (n = 5), *UAS-Fra⊿P1* (n = 3), *UAS-Fra⊿P1⊿P2* (n = 5) significantly rescues the targeting defect seen in *fra*$^{3}$/*fra*$^{4}$ mutant larvae, whereas introduction of *UAS-Fra⊿P3* (n = 5) does not. *109(2)80-Gal4* was used as a driver in these experiments.

Data sets are presented in box plots as median (thick line), quartiles Q1–Q3 (25%–75% quantiles; shaded box), and data in 1.5× quartile range (dashed bars). Data points outside these ranges are indicated as open circles. In (E), *$p < 0.05$ by Wilcoxon rank-sum test (no further delineations of significance are presented for clarity of presentation). *$p < 0.05$; **$p < 0.01$; ***$p < 0.001$ by Wilcoxon rank-sum test. All scale bars represent 50 μm. See also Figure S2.

arborization) in *fra* mutant neurons (Figure 2E). By contrast, anterior coverage was reduced and arborization toward LF was increased in *Dscam1* mutant neurons (Figure 2E). Loss of anterior coverage could reflect an early role for Dscam1 in segregation of anterior and posterior processes [5] or Dscam1-mediated responses to other, nonnetrin, extrinsic cues. Thus, Frazzled and Dscam1 are both required for proper anterior-posterior positioning of ddaA sensory arbors, but with opposite polarities. Removing activity of both Dscam1 and Frazzled diminished both anterior and posterior regions of the arbor, and territory footprints were strongly reduced relative to wild-type (Figures 2D and 2E; Figure S2A). The simplest interpretation of these phenotypes is that Dscam1 and Frazzled have separable functions in dendritic targeting. It appears that Frazzled promotes directional spreading of dendrites, presumably to sources of guidance cues near LF, whereas

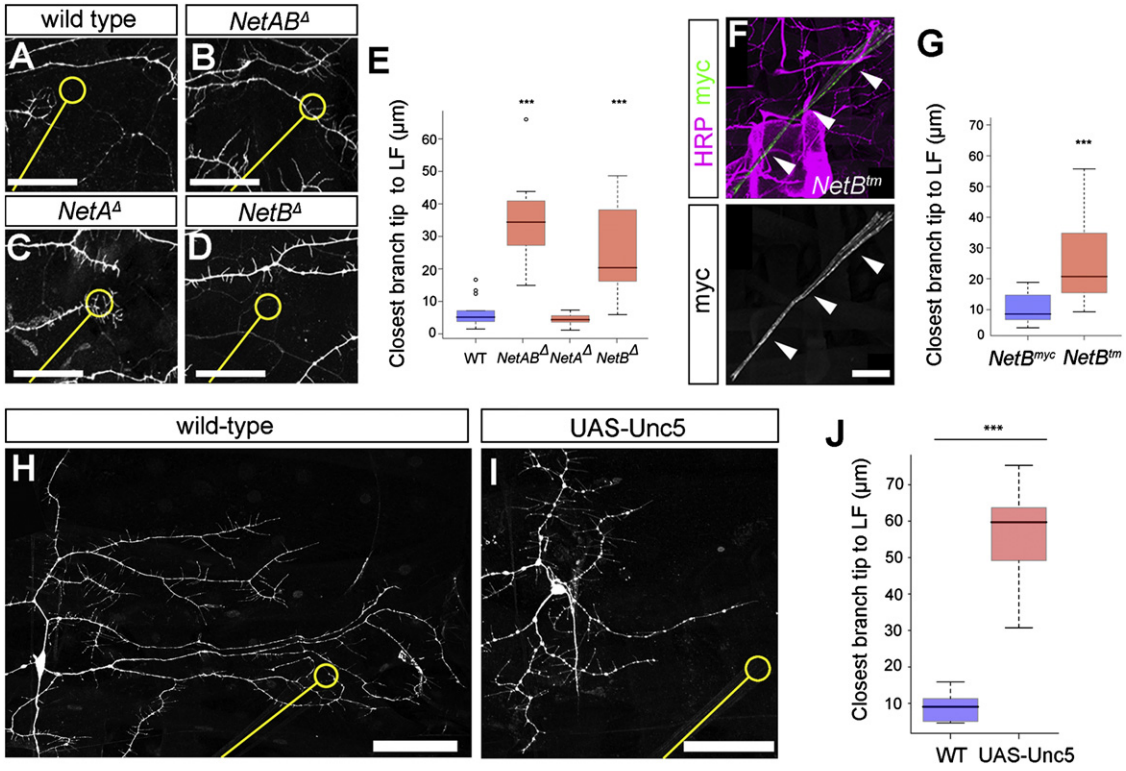


Figure 3. Function of Netrins in Peripheral Dendritic Targeting and Expression of Netrin-B

(A–D) Analysis of targeting of class III da neuron ddaA (marked by *189Y-Gal4, UAS-mCD8::GFP*) in WT (n = 13) (A), *NetAB*$^{\Delta}$ (n = 7) (B), *NetA*$^{\Delta}$ (n = 7) (C), and *NetB*$^{\Delta}$ (n = 13) (D) third-instar larvae. (A)–(D) show representative images of area surrounding LF. The location of the chordotonal organ, labeled in the HRP channel (not shown), is indicated by a yellow line, and the region corresponding to LF is indicated by a yellow circle. Targeting is disrupted in *NetAB*$^{\Delta}$ and *NetB*$^{\Delta}$ mutant larvae.

(E) The distances of the closest major branch tip to LF in WT, *NetAB*$^{\Delta}$, *NetA*$^{\Delta}$, and *NetB*$^{\Delta}$ animals are shown.

(F) NetB$^{tm}$ levels are highly enriched in the chordotonal organ of third-instar larvae (arrowheads).

(G) Quantification of closest tip to LF in *ΔNetA,NetB*$^{myc}$ (n = 10) and *ΔNetA,NetB*$^{tm}$ (n = 17) larvae is shown.

(H) Morphology and chordotonal organ targeting of single wild-type FLP-out clone of ddaA are shown.

(I) Lack of chordotonal targeting of ddaA neuron as revealed by a single FLP-out clone expressing Unc5 under the control of *109(2)80-Gal4* is shown.

(J) Plot of the closest branch tip to LF in wild-type (n = 10) and *UAS-Unc5*-expressing (n = 6) ddaA neurons is shown.

All scale bars represent 50 μm. Data sets are presented in box plots as median (thick line), quartiles Q1–Q3 (25%–75% quantiles; shaded box), and data in 1.5× quartile range (dashed bars). Data points outside these ranges are indicated as open circles. *p < 0.05; **p < 0.01; ***p < 0.001 by Wilcoxon rank-sum test. See also Figure S3.

Dscam1 controls territory positioning by promoting dendrite separation and counterbalancing Frazzled-mediated targeting activity through branch-branch repulsion.

We next performed misexpression experiments to identify the domains of Frazzled that are required for precise dendritic targeting. Overexpression of full-length Frazzled in otherwise wild-type neurons did not alter branch targeting at LF (Figure 2F; Figure S2B). By contrast, misexpression of *FraΔC*, which lacks the cytoplasmic tail and acts as a dominant negative [26], strongly suppressed targeting (Figure 2F; Figure S2B). Three conserved domains within the Frazzled cytoplasmic tail—P1, P2, and P3—are differentially required for axon guidance downstream of Frazzled but have not been examined for activity in dendrite targeting [24, 26, 27]. We assessed requirements in dendrites by testing the ability of Frazzled transgenes lacking different combinations of these domains to rescue *fra* mutant dendrite targeting phenotypes [26]. Transheterozygous *fra*$^{3}$/*fra*$^{4}$ mutant larvae showed deficits in targeting similar to those seen in *fra* MARCM clones (Figure 2G). Targeting was rescued by full-length *UAS-Fra-myc*, *UAS-FraΔP1-myc*, and *UAS-FraΔP1ΔP2-myc* (Figure 2G). By contrast, *UAS-FraΔP3-myc* did not significantly restore targeting in *fra*$^{3}$/*fra*$^{4}$ mutant larvae (p > 0.05, Figure 2G). We observed qualitatively similar levels of expression of the different transgenes (data not shown). Thus, sequences within the P3 domain of Frazzled, but not within P1 or P2, appear to be important for dendritic targeting.

## Netrin-B Is Essential for Frazzled-Dependent Sensory Dendrite Targeting

Two closely related *Drosophila* netrins are encoded by the *Netrin-A* (*NetA*) and *Netrin-B* (*NetB*) genes [28, 29]. We analyzed targeting in larvae lacking one or both netrins using *189Y-Gal4 > UAS-mCD8::GFP* to label class III neurons. Targeting to LF in *189Y-Gal4 > UAS-mCD8::GFP* animals was robust (Figures 3A and 3E) but was strongly disrupted in *NetAB*$^{\Delta}$ mutant animals (Figures 3B and 3E), implicating netrins in precise targeting. We examined dendrite targeting in mutant animals lacking either *Netrin* gene alone and found that NetB, but not NetA, is required for targeting (Figures 3C–3E). Dendrite targeting in *NetAB*$^{\Delta}$ mutant larvae was not significantly different from *fra*$^{3}$/*fra*$^{4}$ mutants (p > 0.05),

suggesting that the activity of netrins during targeting occurs largely, or exclusively, through Frazzled.

We next assessed *NetB* expression in animals carrying a modified *NetB* locus that generates a transmembrane tethered NetB protein tagged with c-*myc* (NetB$^{tm}$) [20]. NetB$^{tm}$ reflects endogenous NetB distribution in the central nervous system but because it is not secreted is more closely associated with membranes of cells in which it is produced [20]. NetB$^{tm}$ was enriched in scolopale cells of LCHO in late embryos (Figure S3A) and accumulated in LCHO cap cells in both abdominal and thoracic segments throughout all larval stages (Figure 3F; Figures S3B–S3D). By contrast, using in situ hybridization, we detected NetA at segment borders (Figure S3E; [29]) but not in LCHO. Notably, dendritic targeting to LF was disrupted in *ΔNetA NetB$^{tm}$* larvae compared to *ΔNetA NetB$^{myc}$* controls (Figure 3G). Targeting was not significantly different in *ΔNetA NetB$^{tm}$* animals compared to *NetAB$^{Δ}$* null animals ($p > 0.05$), together suggesting that secretion of NetB is required for targeting. These data suggest that LCHO cap cells provide the source of secreted NetB that underlies da neuron dendrite targeting.

Although NetA was dispensable for LF targeting, we cannot exclude a role for NetA in da neuron dendritic patterning outside of LF. Notably, we found that misexpression of Unc5, a repulsive netrin receptor [23], in all da neurons using *109(2)80-Gal4* caused defects in dendritic morphology, including disruption of LF targeting (Figures 3H–3J) and aberrant exclusion of dendrites from segment boundaries (Figures S3F and S3G). These results raise the possibility that other sources of netrins, perhaps including NetA at segment borders, could also be important for da neuron dendrite patterning.

### Ectopic Expression of Netrin Directs Dendritic Targeting and Reshapes Sensory Neuron Territories in a Frazzled-Dependent Manner

To test whether localized netrin expression is also sufficient for da neuron dendrite targeting and to further test the respective roles of Dscam1 and Frazzled, we developed an ectopic targeting assay. We used *8-183-Gal4* to drive netrin expression in larval oenocytes, which are clusters of 5 to 6 large hepatocyte-like cells in the lateral body wall [30]. We assessed directional growth of the ddaA dendritic arbor by measuring the relative enrichment of dendrites in either the LF quadrant posterior to the cell body or an adjacent "oenocyte" quadrant directly ventral to the cell body (Figures 4A–4D). Wild-type ddaA dendrites were polarized toward LF and projected more branches to the LF quadrant than the oenocyte quadrant (Figures 4A and 4B). *NetB* misexpression in the oenocytes (*8-183-Gal4 > NetB*) did not significantly alter LF quadrant arborization (Figures 4B and 4D; Figure S4A); however, in the oenocyte quadrant, overall branch number and proportion of arbor increased relative to control, whereas the median distance of the closest branch to the oenocytes decreased (Figures 4B and 4D; Figures S4A and S4B). Both NetA and NetB had qualitatively similar effects on dendritic targeting in this assay (Figure S4C), suggesting that the selective endogenous role for NetB arises as a result of differential expression rather than differential activity. Dendritic territories of ddaA failed to adjust toward ectopic sources of NetB in *fra* mutant larvae (Figures 4E and 4F). Furthermore, although we did not find evidence for dendrite accumulation at the oenocytes in *Dscam1* mutant larvae (Figure 4G) or in density plots generated from mutant clones (Figure 1H), *8-183-Gal4* driving NetB induced dendritic accumulation at oenocytes in larvae mutant for *Dscam1* (Figure 4H). Thus, localized expression of netrins in peripheral tissue was sufficient to direct the targeting of dendrites and reshape arbor territories, and dendrites from a single cell appeared able to respond to multiple such cues. Because opposite patterning defects arose when guidance activity was provided in the absence of Frazzled or Dscam1, our data support a role for Frazzled in attractive responses to netrin and a role for Dscam in self-repulsion and counterbalancing of Frazzled-dependent attraction in normal and ectopic targeting.

### Conclusions

Dendritic targeting is an important component of neural circuit assembly in diverse systems [25, 31–35]. Our data suggest that targeting cues can generate a patterning problem for complex dendrites that must be overcome by self-avoidance signaling. Our findings together suggest a model in which repulsive self-avoidance counters netrin-based attractive signals to permit both precise targeting and full and even territory coverage by sister dendrites. Dendritic branches will be repelled only when their number at any given target becomes excessive. We suggest that control of dendritic targeting by a combination of attractive and self-repulsive cues provides a system for the regulation of branch positioning and spacing that can be implemented dynamically in growing dendrites, and without regard for the exact number and position of guidance cue sources. Indeed, our overexpression results suggest that one advantage of this mechanism is that counterbalancing can be executed in response to multiple, spatially distinct, targeting cues impinging on a single arbor. Conceivably, such action could greatly diversify the shapes taken by dendritic fields. It is worth noting that, in da neurons, counterbalancing is implemented in arbors that are largely restricted to two-dimensional growth. However, in a similar fashion, Dscam1 appears to prevent local accumulations of dendritic and axonal arbors in regions of the brain where arbors elaborate in three dimensions [5, 8]. These observations raise the possibility that repulsive self-avoidance functions as a counterbalancing cue more broadly, perhaps revealing a general role for Dscam1-based self-recognition and repulsion during the formation of neural circuits.

Recent work has shown that Dscams mediate self-avoidance in *Drosophila* and mammals. In *Drosophila*, discrimination between self and nonself dendrites depends on extensive alternative splicing of the Dscam1 ectodomain and selective binding between identical isoforms [15, 16, 36]. Other *Drosophila* Dscams, as well as vertebrate DSCAM, lack the same degree of molecular diversity but nevertheless appear to prevent inappropriate associations and fasciculation between like-type isoneuronal or heteroneuronal processes. *Drosophila* Dscam2 mediates axonal tiling and prevents inappropriate pairings of like-type postsynaptic elements in the visual system [37, 38]. Vertebrate DSCAM and the related DSCAML1 prevent neurite fasciculation and clumping of cell bodies in classes of amacrine cells and retinal ganglion cells [12, 39]. DSCAM and DSCAML1 have been proposed to function in mammalian neurons to mask as yet unknown cell-type-specific adhesive cues that promote clumping and fasciculation of processes [12, 39]. An important future goal is to understand how these opposing cues are integrated by dendrites or axons. In sensory neurons, the integration of self-avoidance and targeting cues is apparently biased in favor of repulsion because the initiation of Dscam1-mediated

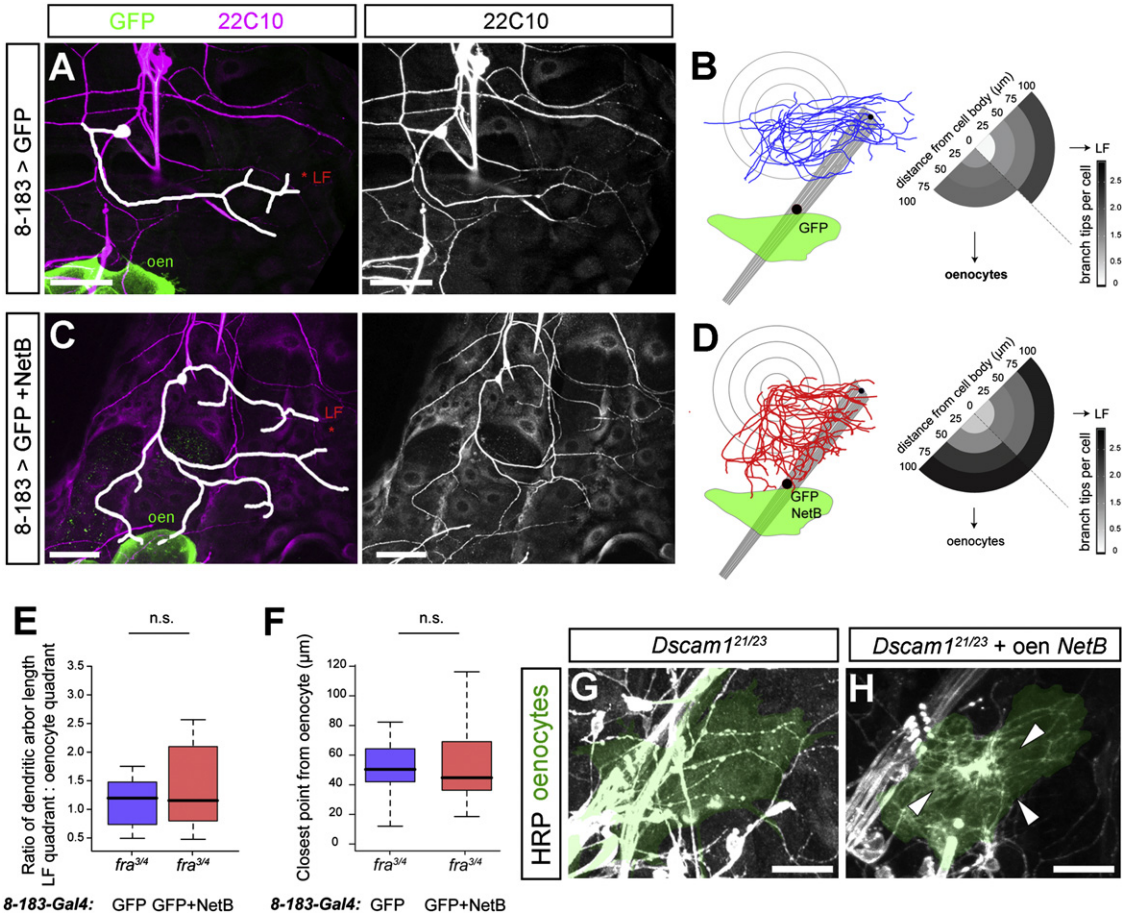


Figure 4. Ectopic Expression of Netrin-B Generates New Dendritic Targets

(A) The dendritic arbor of ddaA in a wild-type larva, visualized by anti-Futsch/22C10 staining. The ventral and posterior portion of the arbor of ddaA is traced in white. *mCD8::GFP* (GFP) is expressed in oenocytes (oen) driven by *8-183-Gal4*.

(B) A plot of multiple registered ddaA arbors (n = 12) with concentric circles placed 25, 50, 75, and 100 μm from the cell body. Dendritic intersections were segregated into two quadrants, one centered toward LF (LF quadrant) and one centered toward the oenocytes (oenocyte quadrant).

(C) Dendritic arbor morphology of ddaA upon expression of mCD8::GFP and NetB under the control of *8-183-Gal4.*

(D) A plot of ddaA dendritic arbors (n = 12) upon misexpression of mCD8::GFP and NetB in the oenocytes. Dendrites are plotted as in (B).

(E) Quantification of the ratio of total arbor length within the quadrant centered on LF and the quadrant centered on the oenocytes reveals no change when NetB is expressed under the control of *8-183-Gal4* in $fra^3/fra^4$ animals.

(F) Quantification of the closest point of each arbor to the oenocytes reveals no change when NetB is expressed under the control of *8-183-Gal4* in $fra^3/fra^4$ animals.

(G) Dendrites do not accumulate at oenocytes (shaded in green) in $Dscam1^{21}/Dscam1^{23}$ mutant larvae (n = 3 animals examined).

(H) Dendrites accumulate at oenocytes (arrows) in $Dscam1^{21}/Dscam1^{23}$ mutant larvae when NetB is expressed under the control of *8-183-Gal4* (n = 6 animals examined).

All scale bars represent 50 μm. Data sets are presented in box plots as median (thick line), quartiles Q1–Q3 (25%–75% quantiles; shaded box), and data in 1.5× quartile range (dashed bars). *p < 0.05; **p < 0.01; ***p < 0.001 by Wilcoxon rank-sum test. See also Figure S4.

self-avoidance appears nonpermissive for Frazzled-dependent branch targeting.

In da neuron dendrite targeting, roles for Dscam1 appear to be separable from those for netrin and Frazzled, because several of our experiments support roles for Dscam1 in self-avoidance and netrin together with Frazzled in attractive guidance. In addition to Frazzled/DCC, Dscam1 in *Drosophila* and DSCAM in mammals have been shown to act as receptors for netrins during axon guidance [17–19]. In the *Drosophila* central nervous system, dendritic attraction by the action of netrins appears to depend largely, or entirely, on Frazzled [34], similar to our findings for da neurons. NetA and Frazzled also instruct the development of the v'ch1 chordotonal organ cap cell, which, in turn, influences dendrite orientation of associated chordotonal neurons [40].

Our results demonstrate how analysis of *Dscam1* mutant phenotypes can uncover new sources of signals that affect neurite patterning. Evidence for targeting cues acting on complex dendrites may be difficult to detect because of the dispersed nature of many dendritic fields and constraints imposed by other cues that may exclude arborization, such as repulsive self-avoidance and tiling. Interfering with self-avoidance appears to provide one approach for identifying preferred targets of neurites, which may then be interrogated further to identify patterning cues for highly branched dendritic arbors. The precision of targeting shown by da neuron

dendrites should prove useful for dissecting signaling mechanisms of targeting and self-avoidance.

### Supplemental Information

Supplemental Information includes four figures and Supplemental Experimental Procedures and can be found with this article online at doi:10.1016/j.cub.2011.07.040.

### Acknowledgments

We are grateful to O. Hobert, L. Zipursky, and members of the Grueber laboratory for comments on earlier versions of the manuscript and for discussions; M. Corty for contributing to Unc5 overexpression experiments; and E. Pyronneau for help with early work on this project. We thank G. Bashaw, B. Dickson, U. Heberlein, F. Roegiers, R. Yang, L. Zipursky, and the Bloomington Stock Center for providing fly stocks and reagents. The 22C10 antibody developed by S. Benzer and the CF.6G11 antibody developed by D. Brower were obtained from the Developmental Studies Hybridoma Bank developed under the auspices of the National Institute of Child Health and Human Development and maintained by the University of Iowa, Department of Biology. B.J.M. was supported by National Institutes of Health (NIH) Predoctoral Fellowship F31NS060341. This work was supported by NIH grant NS061908 from the National Institute of Neurological Disorders and Stroke, the Searle Scholars Program, the Klingenstein Foundation, and the McKnight Endowment Fund (to W.B.G.).

Received: May 24, 2011
Revised: July 26, 2011
Accepted: July 27, 2011
Published online: August 25, 2011

### References

1. Grueber, W.B., and Sagasti, A. (2010). Self-avoidance and tiling: Mechanisms of dendrite and axon spacing. Cold Spring Harb Perspect Biol *2*, a001750.
2. Cameron, S., and Rao, Y. (2010). Molecular mechanisms of tiling and self-avoidance in neural development. Mol. Brain *3*, 28.
3. Schmucker, D., Clemens, J.C., Shu, H., Worby, C.A., Xiao, J., Muda, M., Dixon, J.E., and Zipursky, S.L. (2000). Drosophila Dscam is an axon guidance receptor exhibiting extraordinary molecular diversity. Cell *101*, 671–684.
4. Zhan, X.L., Clemens, J.C., Neves, G., Hattori, D., Flanagan, J.J., Hummel, T., Vasconcelos, M.L., Chess, A., and Zipursky, S.L. (2004). Analysis of Dscam diversity in regulating axon guidance in Drosophila mushroom bodies. Neuron *43*, 673–686.
5. Wang, J., Zugates, C.T., Liang, I.H., Lee, C.H., and Lee, T. (2002). Drosophila Dscam is required for divergent segregation of sister branches and suppresses ectopic bifurcation of axons. Neuron *33*, 559–571.
6. Wang, J., Ma, X., Yang, J.S., Zheng, X., Zugates, C.T., Lee, C.H., and Lee, T. (2004). Transmembrane/juxtamembrane domain-dependent Dscam distribution and function during mushroom body neuronal morphogenesis. Neuron *43*, 663–672.
7. Hattori, D., Demir, E., Kim, H.W., Viragh, E., Zipursky, S.L., and Dickson, B.J. (2007). Dscam diversity is essential for neuronal wiring and self-recognition. Nature *449*, 223–227.
8. Zhu, H., Hummel, T., Clemens, J.C., Berdnik, D., Zipursky, S.L., and Luo, L. (2006). Dendritic patterning by Dscam and synaptic partner matching in the Drosophila antennal lobe. Nat. Neurosci. *9*, 349–355.
9. Matthews, B.J., Kim, M.E., Flanagan, J.J., Hattori, D., Clemens, J.C., Zipursky, S.L., and Grueber, W.B. (2007). Dendrite self-avoidance is controlled by Dscam. Cell *129*, 593–604.
10. Soba, P., Zhu, S., Emoto, K., Younger, S.H., Yang, S.J., Yu, H.-H., Lee, T., Jan, L.Y., and Jan, Y.-N. (2007). Drosophila sensory neurons require Dscam for dendritic self-avoidance and proper dendritic field organization. Neuron *54*, 403–416.
11. Hughes, M.E., Bortnick, R., Tsubouchi, A., Bäumer, P., Kondo, M., Uemura, T., and Schmucker, D. (2007). Homophilic Dscam interactions control complex dendrite morphogenesis. Neuron *54*, 417–427.
12. Fuerst, P.G., Bruce, F., Tian, M., Wei, W., Elstrott, J., Feller, M.B., Erskine, L., Singer, J.H., and Burgess, R.W. (2009). DSCAM and DSCAML1 function in self-avoidance in multiple cell types in the developing mouse retina. Neuron *64*, 484–497.
13. Grueber, W.B., Jan, L.Y., and Jan, Y.-N. (2002). Tiling of the Drosophila epidermis by multidendritic sensory neurons. Development *129*, 2867–2878.
14. McIver, S.B. (1985). Mechanoreception. In Comprehensive Insect Physiology, Biochemistry and Pharmacology, G.A. Kerkut and L.I. Gilbert, eds. (Oxford: Pergamon), pp. 71–132.
15. Wojtowicz, W.M., Flanagan, J.J., Millard, S.S., Zipursky, S.L., and Clemens, J.C. (2004). Alternative splicing of Drosophila Dscam generates axon guidance receptors that exhibit isoform-specific homophilic binding. Cell *118*, 619–633.
16. Wojtowicz, W.M., Wu, W., Andre, I., Qian, B., Baker, D., and Zipursky, S.L. (2007). A vast repertoire of Dscam binding specificities arises from modular interactions of variable Ig domains. Cell *130*, 1134–1145.
17. Andrews, G.L., Tanglao, S., Farmer, W.T., Morin, S., Brotman, S., Berberoglu, M.A., Price, H., Fernandez, G.C., Mastick, G.S., Charron, F., and Kidd, T. (2008). Dscam guides embryonic axons by Netrin-dependent and -independent functions. Development *135*, 3839–3848.
18. Liu, G., Li, W., Wang, L., Kar, A., Guan, K.-L., Rao, Y., and Wu, J.Y. (2009). DSCAM functions as a netrin receptor in commissural axon pathfinding. Proc. Natl. Acad. Sci. USA *106*, 2951–2956.
19. Ly, A., Nikolaev, A., Suresh, G., Zheng, Y., Tessier-Lavigne, M., and Stein, E. (2008). DSCAM is a netrin receptor that collaborates with DCC in mediating turning responses to netrin-1. Cell *133*, 1241–1254.
20. Brankatschk, M., and Dickson, B.J. (2006). Netrins guide Drosophila commissural axons at short range. Nat. Neurosci. *9*, 188–194.
21. Chan, S.S., Zheng, H., Su, M.W., Wilk, R., Killeen, M.T., Hedgecock, E.M., and Culotti, J.G. (1996). UNC-40, a C. elegans homolog of DCC (Deleted in Colorectal Cancer), is required in motile cells responding to UNC-6 netrin cues. Cell *87*, 187–195.
22. Keino-Masu, K., Masu, M., Hinck, L., Leonardo, E.D., Chan, S.S., Culotti, J.G., and Tessier-Lavigne, M. (1996). Deleted in Colorectal Cancer (DCC) encodes a netrin receptor. Cell *87*, 175–185.
23. Keleman, K., and Dickson, B.J. (2001). Short- and long-range repulsion by the Drosophila Unc5 netrin receptor. Neuron *32*, 605–617.
24. Kolodziej, P.A., Timpe, L.C., Mitchell, K.J., Fried, S.R., Goodman, C.S., Jan, L.Y., and Jan, Y.N. (1996). Frazzled encodes a Drosophila member of the DCC immunoglobulin subfamily and is required for CNS and motor axon guidance. Cell *87*, 197–204.
25. Suli, A., Mortimer, N., Shepherd, I., and Chien, C.-B. (2006). Netrin/DCC signaling controls contralateral dendrites of octavolateralis efferent neurons. J. Neurosci. *26*, 13328–13337.
26. Garbe, D.S., O'Donnell, M., and Bashaw, G.J. (2007). Cytoplasmic domain requirements for Frazzled-mediated attractive axon turning at the Drosophila midline. Development *134*, 4325–4334.
27. Dorsten, J.N., and VanBerkum, M.F.A. (2008). Frazzled cytoplasmic P-motifs are differentially required for axon pathway formation in the Drosophila embryonic CNS. Int. J. Dev. Neurosci. *26*, 753–761.
28. Harris, R., Sabatelli, L.M., and Seeger, M.A. (1996). Guidance cues at the Drosophila CNS midline: Identification and characterization of two Drosophila Netrin/UNC-6 homologs. Neuron *17*, 217–228.
29. Mitchell, K.J., Doyle, J.L., Serafini, T., Kennedy, T.E., Tessier-Lavigne, M., Goodman, C.S., and Dickson, B.J. (1996). Genetic analysis of Netrin genes in Drosophila: Netrins guide CNS commissural axons and peripheral motor axons. Neuron *17*, 203–215.
30. Gutierrez, E., Wiggins, D., Fielding, B., and Gould, A.P. (2007). Specialized hepatocyte-like cells regulate Drosophila lipid metabolism. Nature *445*, 275–280.
31. Brierley, D.J., Blanc, E., Reddy, O.V., Vijayraghavan, K., and Williams, D.W. (2009). Dendritic targeting in the leg neuropil of Drosophila: The role of midline signalling molecules in generating a myotopic map. PLoS Biol. *7*, e1000199.
32. Furrer, M.-P., Kim, S., Wolf, B., and Chiba, A. (2003). Robo and Frazzled/DCC mediate dendritic guidance at the CNS midline. Nat. Neurosci. *6*, 223–230.
33. Komiyama, T., and Luo, L. (2007). Intrinsic control of precise dendritic targeting by an ensemble of transcription factors. Curr. Biol. *17*, 278–285.
34. Mauss, A., Tripodi, M., Evers, J.F., and Landgraf, M. (2009). Midline signalling systems direct the formation of a neural map by dendritic targeting in the Drosophila motor system. PLoS Biol. *7*, e1000200.
35. Polleux, F., Morrow, T., and Ghosh, A. (2000). Semaphorin 3A is a chemoattractant for cortical apical dendrites. Nature *404*, 567–573.

36. Sawaya, M.R., Wojtowicz, W.M., Andre, I., Qian, B., Wu, W., Baker, D., Eisenberg, D., and Zipursky, S.L. (2008). A double S shape provides the structural basis for the extraordinary binding specificity of Dscam isoforms. Cell *134*, 1007–1018.
37. Millard, S.S., Flanagan, J.J., Pappu, K.S., Wu, W., and Zipursky, S.L. (2007). Dscam2 mediates axonal tiling in the Drosophila visual system. Nature *447*, 720–724.
38. Millard, S.S., Lu, Z., Zipursky, S.L., and Meinertzhagen, I.A. (2010). Drosophila dscam proteins regulate postsynaptic specificity at multiple-contact synapses. Neuron *67*, 761–768.
39. Fuerst, P.G., Koizumi, A., Masland, R.H., and Burgess, R.W. (2008). Neurite arborization and mosaic spacing in the mouse retina require DSCAM. Nature *451*, 470–474.
40. Mrkusich, E.M., Osman, Z.B., Bates, K.E., Marchingo, J.M., Duman-Scheel, M., and Whitington, P.M. (2010). Netrin-guided accessory cell morphogenesis dictates the dendrite orientation and migration of a Drosophila sensory neuron. Development *137*, 2227–2235.